OncoTargets and Therapy

Dovepress
open access to scientific and medical research

Open Access Full Text Article

ORIGINAL RESEARCH

MIIP is downregulated in gastric cancer and its forced expression inhibits proliferation and invasion of gastric cancer cells in vitro and in vivo

This article was published in the following Dove Press journal:
OncoTargets and Therapy

Dan Sun
Yiwei Wang
Shanshan Jiang
Gang Wang
Yan Xin

Laboratory of Gastrointestinal Onco-Pathology, Cancer Institute, The First Affiliated Hospital of China Medical University, Shenyang 110001, Liaoning Province, China

Background: MIIP is associated with cancer progression in various cancers. However, its expression pattern, and associated molecular mechanisms in gastric cancer (GC) progression are still mysterious. We aimed to explore the role of MIIP in proliferation and invasion of GC.

Materials and methods: MIIP expression was evaluated in human GC tissues and cell lines. Public clinical database of GC patients was used to probe the correlation between MIIP expression and prognosis of patients. The effects of forced MIIP expression on GC cells were determined by MTT, cell cycle distribution, colony formation, wound-healing and Transwell assays in vitro, as well as in vivo growth of subcutaneous tumor xenografts and metastasis of xenografted tumors to the lungs in mice. The expressions of GC progression-associated genes, including *HOTAIR*, *MALAT1*, HDAC6, AC-tubulin, and cyclin D1, were assessed by Western blotting or qRT-PCR.

Results: Both GC tissues and GC cell lines had lower MIIP expression. Higher level of MIIP in GC tissues predicts better survival in patients. Ectopic expression of MIIP in GC cell lines BGC823 and HGC27 induced G_0/G_1 cell cycle arrest and inhibited cell proliferation, colony formation, migration and invasion in vitro, as well as the growth of GC xenografts and metastasis of tumors in vivo. Furthermore, overexpression of MIIP suppressed mRNA expressions of HOTAIR and MALAT1, decreased protein expression of HDAC6 and cyclin D1, and elevated AC-tubulin protein expression.

Conclusion: MIIP is a suppressor for GC progression and is a potential therapeutic target for treating GC.

Keywords: MIIP, gastric cancer, proliferation, migration, invasion, metastasis

Introduction

Gastric cancer (GC) is one of the malignant neoplasms in digestive tract. GC has a high incidence and is the fourth cause of cancer-related mortality worldwide with estimated 50% of death in Eastern Asia.[1,2] Patients with GC have a poor prognosis due to its invasiveness and metastatic potential. Current conventional clinical therapy for GC is surgery and chemotherapy, and the 5-year survival rate is still around 20%–30%, although most patients receive most suitable treatments.[3–5] Therefore, there are considerable interests in finding novel biomarkers and illuminating the mechanisms underlying the invasion and metastatic spread of GC.

The migration and invasion inhibitory protein (MIIP), also known as IIp45, was first reported as a tumor suppressor gene in glioma.[6] Previous studies showed that MIIP located in 1p36 chromosome where frequent deletion occurred, and it has low expression in various tumors, including glioma,[6,7] non-small cell lung cancer

Correspondence: Yan Xin
Laboratory of Gastrointestinal Onco-Pathology, Cancer Institute, The First Affiliated Hospital of China Medical University, 155 Nanjing North Street, Heping District, Shenyang 110001, Liaoning Province, China
Tel +86 24 8328 2375
Email yxin@cmu.edu.cn

submit your manuscript | www.dovepress.com
Dovepress
http://dx.doi.org/10.2147/OTT.S173393

(NSCLC),[8] colorectal cancer,[9] endometrial cancer,[10] and breast cancer.[11] Several potential mechanisms have been reported on how MIIP regulates cancers development and progression. Studies revealed that ectopically expressed MIIP markedly inhibited endometrial cancer cell migration and invasion possibly due to the Rac-1-mediated cytoskeleton reorganization.[10] In addition, MIIP-induced decrease of EGFR expression attenuated downstream RAS gene activation and inhibited the MEK signaling pathway to result in the blocking of tumor cell proliferation in non-small cell lung cancer.[8] Moreover, MIIP directly combined with Cdc20 to suppress the APC/C-mediated cyclin B1 degradation and induced the mitotic catastrophe and cell cycle detention in order to impede glioma progression.[7] MIIP also inhibited tumor cells motility through inhibiting HDAC6 as well as activating α-tubulin.[12] HDAC6, identified as a type II HDAC, specifically mediates deacetylation of α-tubulin to induce chemotactic cell movement.[13] Furthermore, HOX transcript RNA (HOTAIR) and metastasis-associated lung adenocarcinoma transcript 1 (MALAT1), two important lncRNAs, have been reported to regulate the progression and metastasis of GC.[14] These two genes are upregulated and serve as prognostic biomarkers in GC.[15,16] However, little is known on the expression pattern of MIIP in GC, and how the expression of MIIP could affect the abovementioned molecules is also unclear.

In this study, we first evaluated the expression levels of MIIP in both clinical GC tissues and GC cell lines. The GC cell lines BGC823 and HGC27 with ectopically expressed MIIP were used for further cytological studies. Then we explored the role and effect of forced expression of MIIP on cell proliferation, colony formation, cell cycle distribution, migration, and invasiveness of GC in vitro and in vivo. To explore the underlying mechanism, we also tested whether and how MIIP expression in GC affects the expression of HOTAIR, MALAT1, HDAC6, AC-tubulin, and cyclin D1. Besides, our further study on public clinical databases with 354 patients demonstrated that higher level of MIIP in gastric tumor tissues predicts better survival. Our study suggests that MIIP plays a suppressor role in GC, and it might be a promising target for treating GC.

Materials and methods

Clinical sample

Between August 2015 and March 2018, 27 patients with newly diagnosed GC were recruited from the First affiliated Hospital of China Medical University, Shenyang, Liaoning Province, China. Paired fresh GC tissues and adjacent normal mucosa samples were immediately collected after surgery and stored in liquid nitrogen container. These patients did not receive chemotherapy or radiotherapy before surgery. Ethical clearance and approval was obtained from the ethics committee of First affiliated Hospital of China Medical University. The study protocol was carefully explained to the participants, and written informed consent was obtained from all participants. All experiments involving clinical samples were conducted in accordance with the Declaration of Helsinki.

Clinicopathological features and prognosis of GC patients

Data on clinicopathological characters of 407 GC patients were downloaded from the Cancer Genome Atlas (https://cancergenome.nih.gov), while data on the survival of 354 GC patients were retrieved from the publicly available database of the Human Protein Atlas (https://www.proteinatlas.org/). As recommended by the website, the cutoff value for distinguishing MIIP-high expression to MIIP-low expression was set as 7 fragments per kilobase of transcript per million mapped reads. The correlation between expression of MIIP mRNA and the clinicopathological characters of 407 GC patients was analyzed by RT-qPCR and histological analyses. The Kaplan–Meier curves were used to show the prognostic differences between the MIIP-low and MIIP-high groups of 354 GC patients, and the statistics were analyzed by using the log-rank test.

Cell culture

The normal human gastric epithelial cell line GES-1 and human GC cell lines BGC823, SGC7901, MKN45, and HGC27 were purchased from Genechem Co., Ltd., Shanghai, China. These cell lines were then preserved in the Gastrointestinal Onco-Pathology Laboratory of China Medical University. Cells were maintained in RPMI1640 medium (Gibco®; Thermo Fisher Scientific, Waltham, MA, USA) supplemented with 10% FBS (Cellmax, Sydney, Australia), 100 units/mL of penicillin, and 100 μg/mL of streptomycin (Gibco®; Thermo Fisher Scientific, Waltham, MA, USA), and grown in a humidified atmosphere with 5% CO_2 at 37°C. The culture medium was changed every other day.

Western blotting

After washing with cold PBS, grinded clinical samples and cell line samples were lysed in radioimmunoprecipitation assay (RIPA; Sigma-Aldrich Co., St Louis, MO, USA) lysis buffer containing a protease and phosphatase inhibitor cocktail on ice for 30 minutes. After centrifugation at 13,000× *g* for 20 minutes at 4°C, proteins in the supernatants

were quantified by a bicinchoninic acid assay (Beyotime, Shanghai, China), and equal amounts of total proteins were loaded. Total proteins were separated by 10% SDS-PAGE and electrophoretically transferred to polyvinylidene fluoride membranes. After blocking, the membranes were incubated with exclusive primary antibodies: rabbit polyclonal anti-MIIP (1:500; BIOSS Co., Ltd., Beijing, China), rabbit polyclonal anti-HDAC6 (1:1,500; Abcam, Cambridge, UK), rabbit monoclonal anti-acetylated α-tubulin (1:1,500; Abcam), and rabbit monoclonal anti-Cyclin D1 (1:1,000; Cell Signaling Technology Company, Boston, MA, USA). Incubation with primary antibodies was followed by the corresponding secondary antibody (1:5,000; Origene Co., Ltd., Shanghai, China). The enhanced chemiluminescence (EMD Millipore, Billerica, MA, USA) kit was used to visualize the proteins of interest. Quantity One software (Bio-Rad Laboratories, Inc., Hercules, CA, USA) was applied to evaluate the blots by grayscale analysis. Western blotting assays of all the experiments were repeated at least three times, and one representative blotting result is shown for each experiment.

Plasmids and transfection

The coding sequences of human MIIP gene (NM_021933.3) was integrated into a pCMV6 plasmid vector (Origene Co., Ltd.) by regular molecular subcloning. When the confluence of BGC823 and HGC27 cells reached at 70%–80%, cells were transfected with this plasmid using Lipofectamine 2000 (Invitrogen). After continuous G418 (800 ng/μL) pressure screening for 2 weeks, cells stably expressing MIIP were selected for expansion. Correspondingly, the pcDNA control vector expressing enhanced green fluorescent protein was used for cell transfection and subsequent G418 pressure screening and propagation of control cells in parallel. The expression of exogenous MIIP was identified by qRT-PCR and Western blotting assays. The cell lines with ectopic expression of MIIP gene were named MIIP/BGC823 cells and MIIP/HGC27 cells, respectively, while the cell lines transfected with the pcDNA control vector were named as GFP/BGC823 cells and GFP/HGC27 cells, respectively.

MTT assay

Exponentially growing cells were trypsinized and seeded into 96-well plates at 2×10^3 cells/well. Cells were respectively incubated for 24, 48, 72, 96, and 120 hours. Following the operation manual, 20 μL MTT reagent was added into the cell culture medium, and cells were incubated for another 4 hours at 37°C. Then the formazan was solubilized with 150 μL dimethyl sulfoxide. The absorbance value was measured at 490 nm by a microplate reader. The viability of cells was monitored for a period of five consecutive days, and this experiment was repeated three times.

Colony formation assay

Cells of each group were planted at a density 2×10^2 cells/well and cultured in six-well plates for 11 days. Cell colonies were stained with 0.1% crystal violet (Sigma-Aldrich Co., USA). The number of colonies foci >50 cells was calculated using an inverted phase contrast microscope (Nikon, Tokyo, Japan). Data presented were obtained from experiments repeated three times.

Flow cytometry (FCM) analysis

The effect of MIIP expression on the cell cycle distribution of GC was analyzed by flow cytometry (FCM). Briefly, the harvested cells were fixed by 70% ethanol in 4°C refrigerator overnight. Then cells were centrifuged and incubated with propidium iodide staining solution (Beyotime) in the dark at 37°C for 30 minutes. Then the cell cycle distribution of GC cells was detected using a FCM analyzer (FACSCalibur; BD Biosciences, San Jose, CA, USA).

Cell invasion and migration assay

The potential of migration and invasion for GC cells was assessed by the 24-well Transwell system (8.0 μm pore size; Corning Incorporated, Corning, NY, USA). In the migration assay, 4×10^4 cells were cultured in 200 μL of serum-free RPMI1640 medium in the upper layer of a noncoated Transwell insert. The under layer of well was filled with 600 μL of RPMI1640 medium supplemented with 20% FBS. For invasion assay, the upper layers of the 24-well Transwell system were first coated with diluted matrix glue (BD Biosciences). Subsequently, 600 μL of RPMI1640 medium with 20% FBS and 4×10^4 cells were added into the well, and cells were incubated for 48 hours. Cells were stained with 0.1% crystal violet (Sigma) and quantified under a microscope (Nikon).

Wound healing assay

Cells were cultured in six-well plates overnight. A wound was made by scraping off the cells in the central region of the wells using a pipette tip when cells reached the confluency of 80%–90%. The drifting cells in six-well plates were washed away and removed by PBS. After cells were replenished with fresh medium, the wound healing status was observed and photographed using a microscopy at 0, 24, and 48 hours. The wound-healing rate was quantitatively evaluated using the software Quantity One (Bio-Rad Laboratories).

qRT-PCR

The EASYspin Plus Kit (Aidlab, Beijing, China) was used to isolate total RNA from tissues and cancer cell lines following the manufacturer's protocols. Total RNA was reversely transcribed into complementary DNA (cDNA) with PrimeScript® RT reagent kit (TaKaRa, Dairen, China). The mRNA expression of targeted genes was quantified by the SYBR® Premix TaqTM I (TaKaRa) and calculated by using the $2^{-\Delta\Delta CT}$ method.[17] The sequences of primers are as follows: MIIP, 5′-ATCTGCAGCCATCCTGAACC-3′ (sense) and 5′-CAGTGTGTCAGAGGCGTCAA-3′ (antisense); HOTAIR, 5′-GGTAGAAAAAGCAACCACGAAGC-3′ (sense) and 5′-ACATAAACCTCTGTCTGTGAGTGCC-3′ (antisense); MALAT1, 5′-TAGGAAGACAGCAGCA GACAGG-3′ (sense) and 5′-TTGCTCGCTTGCTCCTC AGT-3′ (antisense); and GAPDH, 5′-GAAGGTGAAG GT CGGAGTC-3′ (sense) and 5′-GAAGATGGTGATGGG AT TTC-3′ (antisense). The mRNA expression of GAPDH was used as an internal reference.

Mouse tumor models

Twenty female BALB/c-nude mice (weight 18–20 g, 4–6 weeks old) were purchased from Beijing Vital River Laboratory Animal Co., Ltd. (Beijing, China) and randomly divided into BGC823 and MIIP/BGC823 groups. All procedures involving experimental animals were approved by the University Committee on the Use and Care of Animals at First Affiliated Hospital of China Medical University. All animal experiments entirely obeyed the National Animal Care and Ethics Institution. Ten mice were used to establish xenografted tumor model of GCs. About 2×10^6 cells per mouse in 200 μL PBS were implanted subcutaneously into the right subaxillary of each mouse. Other ten mice were intravenously injected with BGC823 or MIIP/BGC823 cells through tail vein at a dose of 5×10^6 cells per mouse. The weight and size of xenografted tumors were measured on the 28th day after cells inoculation. The tumor volume was calculated according to the formula: volume = $a\times b\times b/2$, where a and b represented the longer diameter and shorter diameter, respectively. At 8 weeks after cell injection, the model mice for hematogenous dissemination of GCs were sacrificed. Lungs were removed, fixed, and embedded. The tissue blocks were stained with H&E and then observed using a microscope for counting numbers of metastases.

Statistical analyses

All quantitative data were analyzed with SPSS 17.0 (IBM Corporation, Armonk, NY, USA) and GraphPad Prism 5 (GraphPad Software, Inc., La Jolla, CA, USA). Data for experiments repeated for three times were expressed as mean ± SD. One-way ANOVA was performed for statistical analysis among multiple groups. P-values <0.05 were considered statistically significant.

Results

Human gastric cancer tissues and gastric cancer cell lines exhibited lower expression of MIIP

First, we examined the expression of MIIP in human GC tissues and adjacent normal tissues by Western blotting. As shown in Figure 1A, GC tissues had lower levels of MIIP protein than the matched normal tissues. Statistical analyses also demonstrated significantly ($P<0.05$) downregulated expression of MIIP at protein level (Figure 1B) and mRNA level (Figure 1C) in 27 GC tissues, when comparing with paired normal tissues. We also detect MIIP protein expression in human GC cell lines (BGC823, SGC7901, MKN45, and HGC27) and normal human gastric epithelial cell line (GES-1). The expression of MIIP in GES-1 cells was evidently higher than that in all the GC cells, and BGC823 cells had the lowest expression of MIIP among all cell lines (Figure 1D). These results indicated that MIIP expression was decreased in GC tissues and GC cell lines.

Establishment of BGC823 and HGC27 cell lines with stable expression of MIIP

To investigate the biological function of MIIP, we selected BGC823 and HGC27 GC cell lines, which express much lower level of MIIP among tested cell lines, for transfection of MIIP-expressing plasmid vector. The stable BGC823 and HGC27 cell pools were obtained by screening with G418 drug pressure. Our results from the Western blotting assays verified the expression of MIIP in both BGC823 cells (Figure 1E) and HGC27 cells (Figure 1F). The expression of green fluorescence protein was observed in stable GFP/BGC823 cells transfected with empty vector, MIIP/BGC823 cells transfected with MIIP-expressing vector, GFP/HGC27 cells transfected with empty vector (Figure 1G), and MIIP/HGC27 cells transfected with MIIP-expressing vector (Figure 1G).

Higher level of MIIP in gastric tumor tissues predicts better survival in patients

In order to link our findings to clinical data, we assessed and retrieved the databases on clinicopathological characters and prognosis of patients with GC from the public available databases, and then identified the expression levels of MIIP in cancer tissues. The summary data on clinicopathological characters of 407 patients are shown in Table 1.

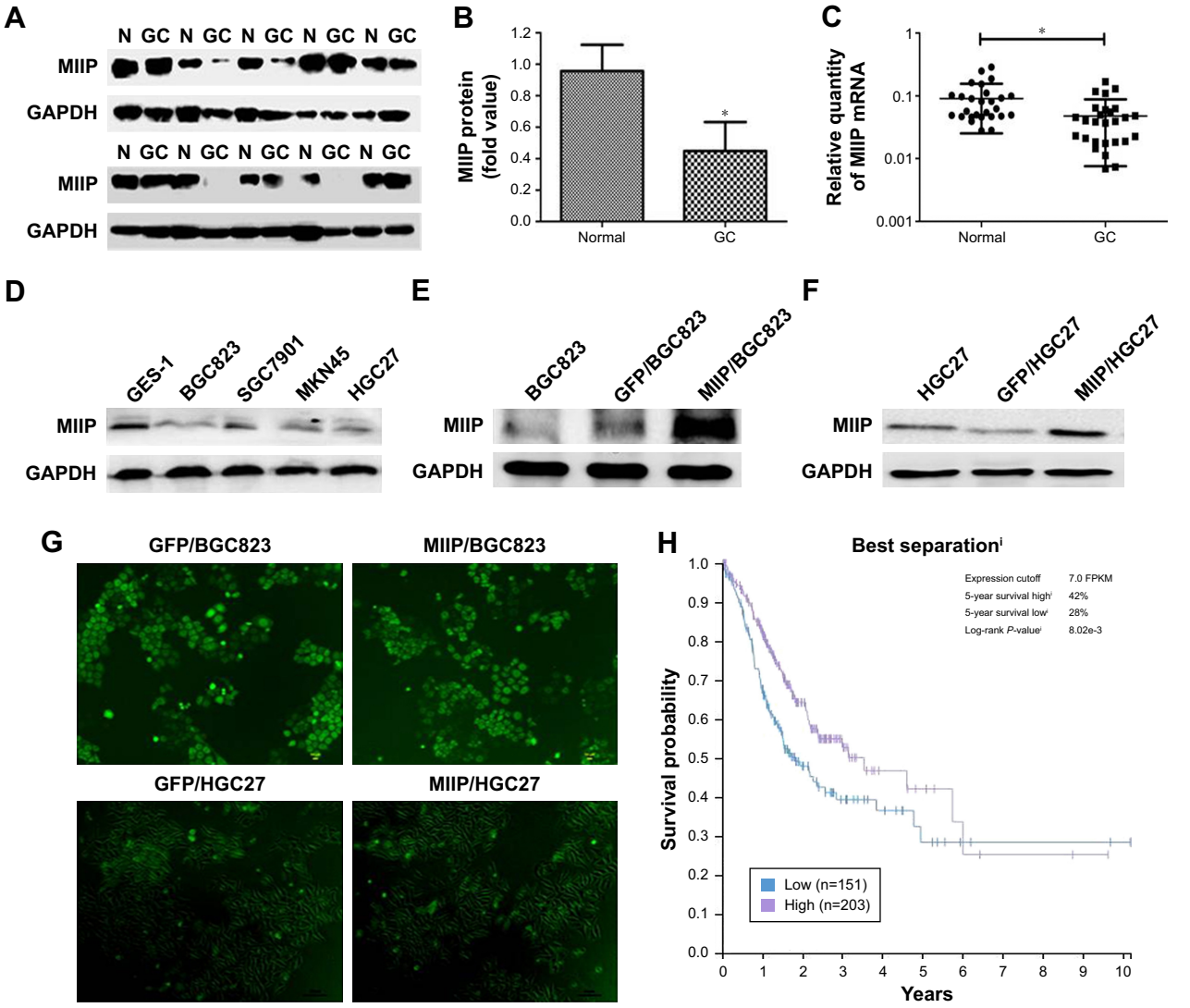

Figure 1 Relative expression of MIIP in human GC tissues and GC cell lines.

Notes: (**A**) Representative Western blotting images showing the expression of MIIP protein in ten GC samples and matched normal mucosa tissues. (**B**) The statistical diagram of MIIP protein expression in 27 paired GC tissues and adjacent normal tissues. (**C**) The statistical diagram of MIIP mRNA expression in 27 paired GC tissues and adjacent normal tissues. *$P<0.05$. (**D**) Detection of the protein expression of MIIP in human gastric carcinoma cell lines (BGC823, SGC7901, MKN45, and HGC27) and human immortalized normal gastric mucosa cell line GES-1 by Western blotting. (**E**, **F**) Representative images of Western blotting assay showing the expression of MIIP in human GC cell lines with stable overexpression of MIIP in BGC823 (**E**) and HGC27 (**F**) cells. BGC823 and HGC27 denote cells without transfection. While GFP/BGC823 and GFP/HGC27 denote cells transfected with GFP-expressing empty vector, MIIP/BGC823 and MIIP/HGC27 denote cells transfected with GFP- and MIIP-coexpressing vector. (**G**) Microscope fluorescent images showing the expression of GFP in BGC823 cells (upper panel) and HGC27 cells (lower panel) transfected with GFP-expressing empty vector (left) or GFP- and MIIP-coexpressing vector (right). (**H**) Higher level of MIIP in gastric tumor tissues predicts better survival in patients, as indicated by Kaplan–Meier analysis. Among 354 patients with GC, lower expression of MIIP was significantly associated with poor overall survival ($P<0.05$). Patients' numbers and cutoff values of MIIP expression are indicated in the figure. While the 5-year survival rate for patients with lower expression of MIIP is 28%, the patients with higher MIIP expression in tumors have a 5-year survival rate of 42%.

Abbreviations: FPKM, fragments per kilobase of transcript per million mapped reads; GC, gastric cancer; MIIP, migration and invasion inhibitory protein.

Low expression of MIIP only correlated to the anatomic neoplasm subdivision, but not to other clinicopathological features such as histology types and TNM staging. However, among 354 GC patients with follow-up information, Kaplan–Meier analysis demonstrated that low expression of MIIP was significantly associated with poor overall survival ($P<0.05$). While the 5-year survival rate for patients with lower expression of MIIP is 28%, the patients with higher MMIP expression in tumors have a 5-year survival rate of 42% (log-rank $P=0.008$; Figure 1H). The data clearly suggest that high expression of MIIP in gastric tumor tissues can predict better survival in patients with GC.

Ectopic expression of MIIP led to proliferation inhibition and G_0/G_1 cell cycle arrest in BGC823 and HGC27 cells

MTT assay was applied to determine whether MIIP had an antiproliferative effect in BGC823 and HGC27 cells.

Table 1 Correlation between MIIP expression and clinicopathological features in gastric cancer

Variables	n	MIIP expression		χ^2	*P*-value
		Low (%)	High		
Age (years)	403			0.027	0.869
≤68	220	104 (47.3)	116		
>68	183	86 (46.4)	98		
Gender	407			0.049	0.824
Female	144	69 (47.9)	75		
Male	263	123 (46.8)	140		
Race	348			3.997	0.262
White	255	119 (46.7)	136		
Black or African American	12	6 (50.0)	6		
Asian	81	33 (40.7)	48		
Anatomic neoplasm subdivision	389			3.956	0.047*
Gastroesophageal junction	47	28 (59.6)	19		
Antrum/distal + fundus/body + cardia/proximal	342	151 (44.2)	191		
Grade	398				0.565#
G1	10	6 (60.0)	4		
G2	150	69 (46.0)	81		
G3	238	111 (71.0)	127		
WHO's histology types	406				0.764#
Papillary type	5	3 (60.0)	2		
Well differentiated tubular adenocarcinoma	144	66 (45.8)	78		
Moderately differentiated tubular adenoma	67	28 (41.8)	39		
Poorly differentiated tubular adenoma	159	79 (49.7)	80		
Signet ring type	11	4 (36.4)	7		
Mucinous type	20	11 (55.0)	9		
Lauren's types	406			0.964	0.618
Intestinal	169	80 (47.3)	89		
Diffuse	170	83 (48.8)	87		
Mixed	67	28 (41.8)	39		
Depth of invasion	399			6.027	0.11
T1	22	13 (59.1)	9		
T2	91	47 (51.6)	44		
T3	181	72 (39.8)	109		
T4	105	52 (49.5)	53		
Lymph node metastasis	388			2.156	0.541
N0	123	51 (41.5)	72		
N1	108	54 (50.0)	54		
N2	83	41 (49.4)	42		
N3	74	33 (44.6)	41		
Distant metastasis	385			0.851	0.356
M0	358	166 (46.4)	192		
M1	27	15 (55.6)	12		
TNM staging	383			4.381	0.223
I	59	30 (50.8)	29		
II	126	49 (38.9)	77		
III	156	72 (46.2)	84		
IV	42	23 (54.8)	19		

Note: #Fisher's exact test. *$P<0.05$.
Abbreviation: MIIP, migration and invasion inhibitory protein.

In the first 4 days of culturing, no significant differences of cell viabilities among BGC823, GFP/BGC823, and MIIP/BGC823 groups were observed (Figure 2A), while HGC27, GFP/HGC27, and MIIP/HGC27 groups also demonstrated similar proliferation activity (Figure 2E). However, the cell proliferation in MIIP/BGC823 and MIIP/HGC27 groups was significantly slowed down on the fifth day when comparing to other corresponding control groups ($P<0.05$,

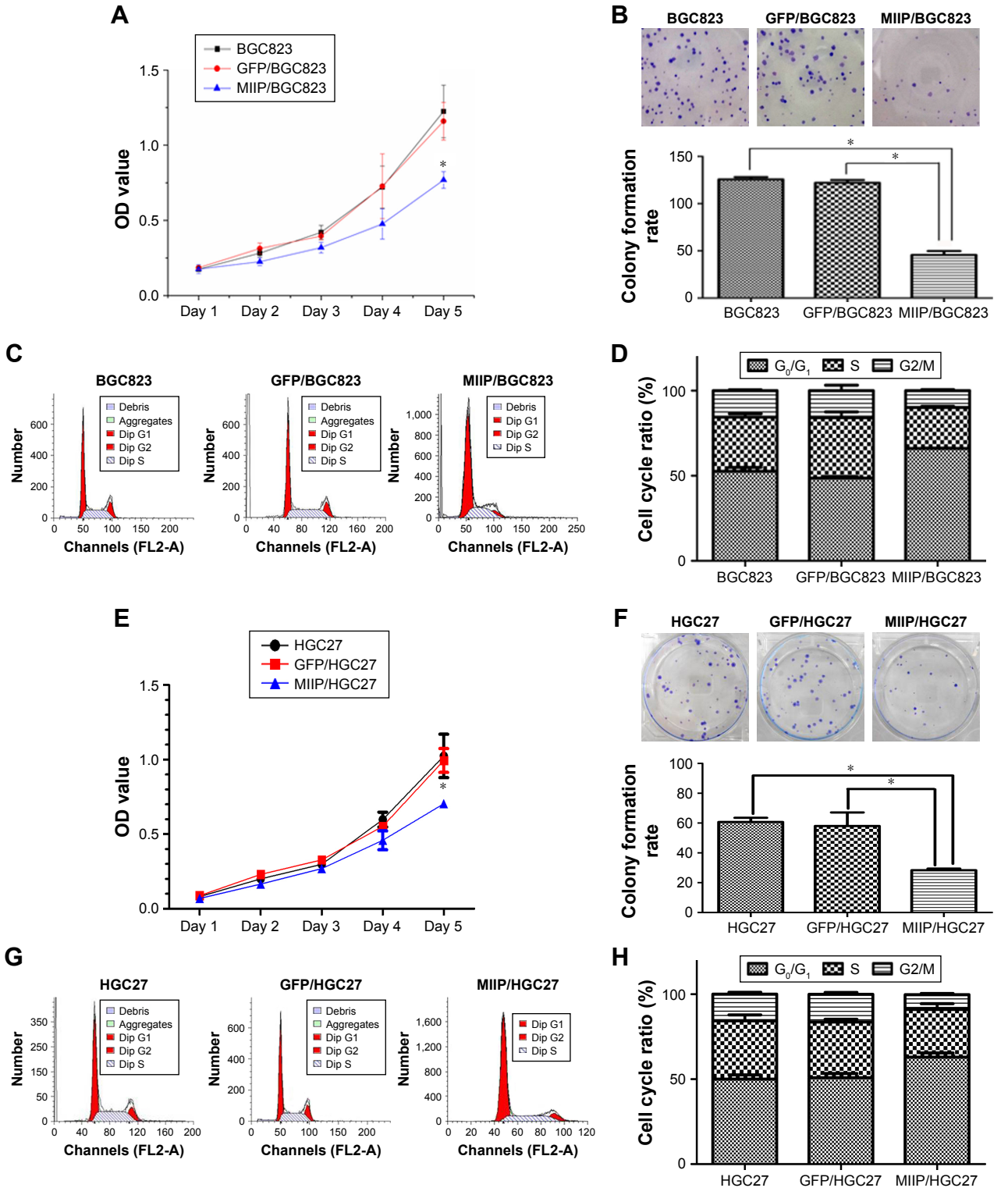

Figure 2 MIIP inhibited the proliferation and colony formation of gastric cancer cells in vitro.

Notes: (**A**) Proliferation curve of BGC823 cells without treatment (BGC823), with stable GFP expression (GFP/BGC823), and with stable MIIP expression (MIIP/BGC823). Data were obtained by MTT assay. (**B**) Representative images showing the colony formation for BGC823, GFP/BGC823 and MIIP/BGC823 cells. The summary data are shown below the images. (**C**, **D**) Representative flow profile showing the distributions of cell cycle phases in BGC823, GFP/BGC823, and MIIP/BGC823 cells. The bar graph shows the summary data on the percentage of cells in different phases (**D**). (**E**) Proliferation curve of HGC27 cells without treatment (HGC27), with stable GFP expression (GFP/HGC27) and with stable MIIP expression (MIIP/HGC27). Data were obtained by MTT assay. (**F**) Representative images showing the colony formation for HGC27, GFP/HGC27, and MIIP/HGC27 cells. The summary data are shown below the images. (**G**, **H**) Representative flow profile showing the distributions of cell cycle phases in HGC27, GFP/HGC27, and MIIP/HGC27 cells. The bar graph shows the summary data on the percentage of cells in different phases (**H**). n=3 for each group; *$P<0.05$.

Abbreviation: MIIP, migration and invasion inhibitory protein.

Figure 2A and E). Since elevated colony formation capacity also means malignant tumor progression, which is a typical characteristic of GC cells, we performed this assay to identify the impact of MIIP expression on the malignancy of gastric carcinoma cells. Notably, forced expression of MIIP in the MIIP/BGC823 (Figure 2B) and MIIP/HGC27 (Figure 2F) cells significantly impaired the colony formation abilities of these gastric carcinomas.

To further elucidate the mechanisms by which MIIP negatively regulated proliferation in GC cells, we assessed the effects of MIIP expression on cell cycles in BGC823 and HGC27 cells by flow cytometric analysis. As shown in Figure 2C and G, the percentages of MIIP/BGC823 and MIIP/HGC27 cells in G_0/G_1 phase were upregulated while percentages of cells in S and G2/M phase were obviously downregulated, compared with BGC823, GFP/BGC823, HGC27, and GFP/HGC27 cells in the control groups (statistical columns are shown in Figure 2D and H). Taking together, our results demonstrated that ectopic expression of MIIP induced G_0/G_1 cell cycle arrest in both BGC823 and HGC27 cells.

Ectopic expression of MIIP suppressed the invasion and migration abilities of BGC823 and HGC27 cells

To measure the effect of MIIP overexpression on the invasion and migration abilities of GC cells, MIIP/BGC823 and MIIP/HGC27 cells were compared with other control cells in Transwell and wound-healing experiments. As shown in Figure 3A and E, the numbers of cells invaded into the lower layer were apparently fewer in MIIP/BGC823 and MIIP/HGC27 groups with MIIP overexpression, than that in BGC823, GFP/BGC823, HGC27, and GFP/HGC27 control groups, respectively. Meanwhile, in the Transwell system plate, fewer MIIP/BGC823 and MIIP/HGC27 cells were migrated and invaded into the under layer than cells in other control groups (Figure 3B and G). In addition, the numbers of MIIP/BGC823 and MIIP/HGC27 cells in the wounded area were significantly decreased (Figure 3C and F). The curves for ratio of wound healing in BGC823 and HGC27 cells also demonstrated that ectopic expression of MIIP delayed the healing of GC cells, and more differences in the numbers of percent of healing ratio were found at the 48-hour time

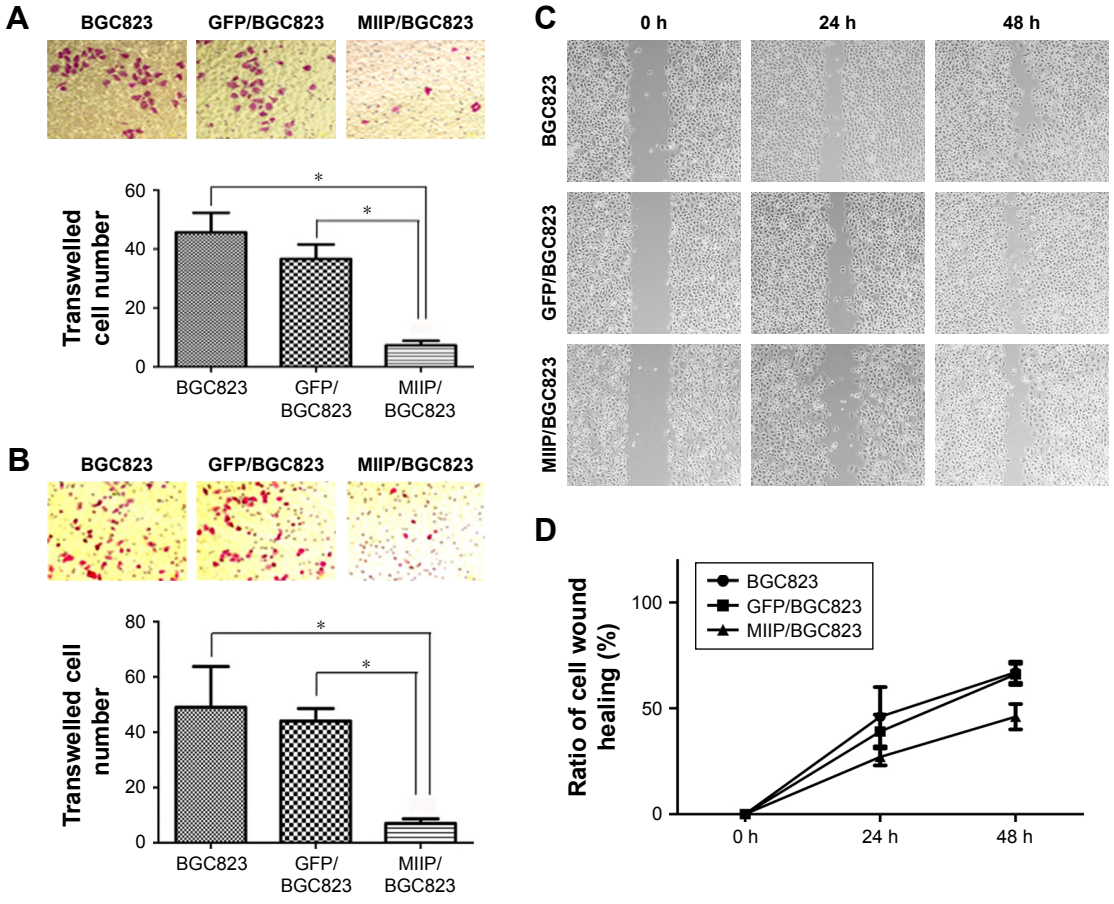

Figure 3 (*Continued*)

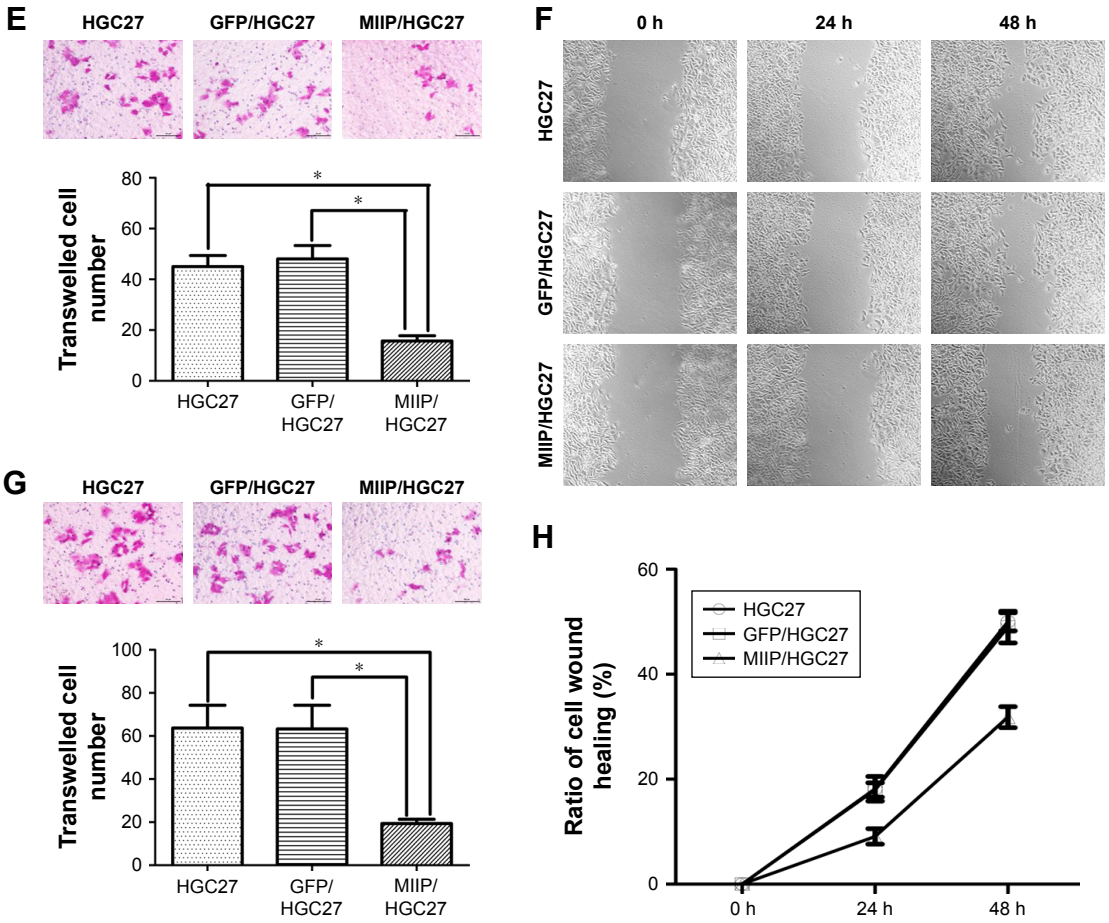

Figure 3 MIIP suppressed the invasion and migration of gastric cancer cells in vitro.

Notes: (**A**, **E**) Representative images showing the cells invading through the Transwell membrane in BGC823 cells (**A**) and HGC27 cells (**E**). Original magnification ×200. The bar graph shows the summary data on numbers of invaded cell. (**B**, **G**) Representative images showing the BGC823 cells (**B**) and HGC27 cells (**G**) migrated to the lower chamber in the Transwell assay. The bar graph shows the summary data on numbers of migrated cells. Original magnification ×200; n=3 for each group; *$P<0.05$. (**C**, **F**) The wound-healing assay was used to evaluate the migration properties of BGC823 (**C**) and HGC27 (**F**) cells. Cells were photographed at 0, 24, and 48 hours after wounding (original magnification ×100). Cells between the wound edges were the cells that migrated to the wound area. (**D**, **H**) The migration ability of cells in the MIIP/BGC823 and MIIP/HGC27 groups was significantly decreased compared with the control groups (n=3 for each group; *$P<0.05$). The curves showed the ratio of cell wound healing from 0 hour to 48 hours. BGC823 and HGC27 denote cells without transfection. While GFP/BGC823 and GFP/HGC27 denote cells transfected with GFP-expressing empty vector, MIIP/BGC823 and MIIP/HGC27 denote cells transfected with GFP- and MIIP-coexpressing vector.

Abbreviation: MIIP, migration and invasion inhibitory protein.

point (Figure 3D and H). All data above clearly indicated that overexpression of MIIP attenuated the invasion and migration abilities of GC cells.

MIIP expression inhibited tumor growth in a xenograft mouse model and lung metastases in a hematogenous dissemination mouse model

In order to explore the effect of MIIP expression on tumor proliferation in vivo, BGC823 and MIIP/BGC823 cells were injected into mouse's right subaxillary region with the subcutaneous inoculation method. The weight and size of the xenografted tumor were measured on 28th day after inoculation. Among the five mice in each group, all the mice in the control BGC823 group bear tumors, while two mice in the MIIP/BGC823 group did not have palpable tumors (Figure 4A and B). The mice inoculated with MIIP-overexpressing BGC823 cells had significantly attenuated tumor growth than the control group, as evidenced by both tumor weight (Figure 4C) and tumor size (Figure 4D). The effect of MIIP expression on invasion and metastasis of GCs to lung was investigated in the hematogenous dissemination mice model by seeding BGC823 or MIIP/BGC823 cells into mice through tail vein injection. The tumor metastasis to lung in mice of MIIP/BGC823 group declined strikingly compared with that in mice of BGC823 group (Figure 5A and B), which was also supported by significantly reduced number of focuses in mice of MIIP/BGC823 group (Figure 5C). Therefore, these results further demonstrated that MIIP played a vital role in

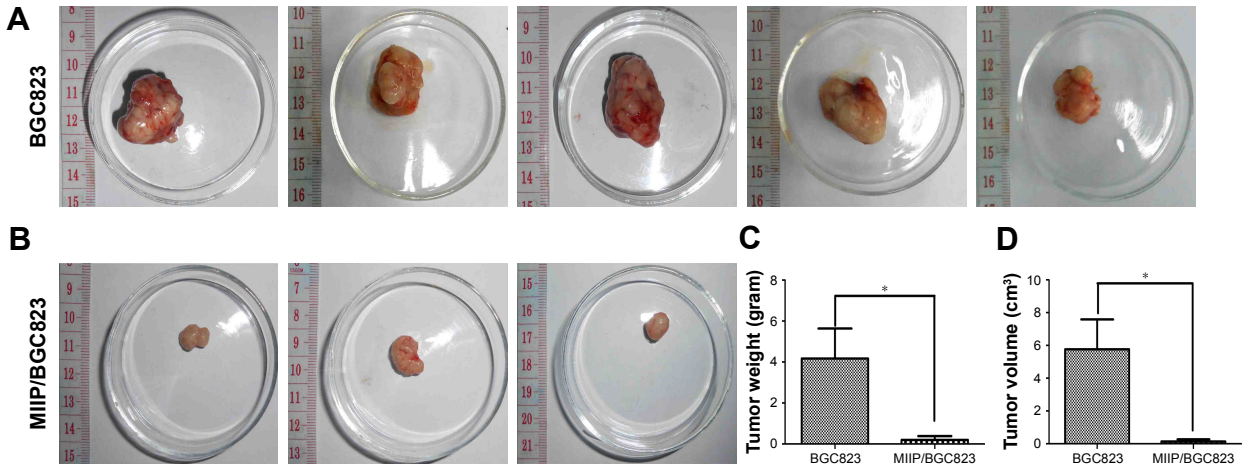

Figure 4 MIIP inhibited the growth of subcutaneously xenografted BGC823 cancer cells in vivo.
Notes: (**A**–**D**) Ten BALB/c-nude mice were intravenously injected with BGC823 or MIIP/BGC823 cells through tail vein at a dose of 5×10^6 cells per mouse (n=5 for each group). Mice were sacrificed on the 28th day after cells inoculation. (**A**) All five mice in the BGC823 group showed transplanted tumors. (**B**) Three of five mice in the MIIP/BGC823 group showed smaller tumors, and the other two mice did not have tumors. (**C**) The average tumor weight in the MIIP/BGC823 group was significantly lower than that in the BGC823 group (*$P<0.05$). (**D**) The average volume of xenografted tumor in MIIP/BGC823 group was obviously smaller than that in the BGC823 group (*$P<0.05$).
Abbreviation: MIIP, migration and invasion inhibitory protein.

the inhibition of xenograft tumor growth and formation of lung metastases.

MIIP negatively regulated the mRNA expression of lncRNAs HOTAIR and MALAT1 in gastric cancer cells

Since the lncRNAs HOTAIR and MALAT1 have been reported to regulate the progression and metastasis of GCs,[14–16] we set out to evaluate the impact of MIIP expression on mRNA levels of HOTAIR and MALAT1 by qRT-PCR. We first identified that the mRNA expression of MIIP was much higher in MIIP/BGC823 cells, which were transfected with MIIP-expressing pasmid (Figure 6A). Whereas, in comparison with control BGC823 and GFP/BGC823 cells, significantly lower expression of HOTAIR mRNA (Figure 6B) and MALAT1 mRNA (Figure 6C) in MIIP/BGC823 cells was identified. These results suggested that elevated expression of MIIP mRNA could induce the decrease of the mRNA expressions of GC-related lncRNAs HOTAIR and MALAT1, which could at least partially contribute to the attenuation of proliferation, invasion, and metastasis of GC cell.

MIIP regulated the protein expressions of HDAC6, AC-tubulin, and cyclin D1 in gastric cancer cells

HDAC6 has been reported to regulate tumor cell migration and invasion, and Wu et al found that MIIP inhibited cell motility by inhibiting HDAC6 expression and increasing intracellular acetylated α-tubulin (AC-tubulin) levels in glioma.[12] To test whether HDAC6 also participate in MIIP overexpression-mediated inhibitory effects on cell migration and invasion in GCs, Western blotting assay was performed to detect protein levels of HDAC6 and AC-tubulin in BGC823, GFP/BGC823, and MIIP/BGC823 cells. Our results revealed that while HDAC6 protein expression was significantly downregulated in MIIP/BGC823 cells, AC-tubulin protein expression was increased, when comparing to other control cells (Figure 6D). Cyclin D1 serves as a cell cycle regulatory switch in actively proliferating cells,[18] and its reduction has been identified to be sufficient to induce G1 cell cycle arrest in cancer cells.[19] Therefore, we also compared the levels of cyclin D1 in GC cells with differential expression of MIIP. As shown in Figure 6E, MIIP/BGC823 cells had evidently lower expression of cycling D1, which can contribute to MIIP overexpression-induced G1 arrest. Taking together, these results demonstrated that MIIP inhibited the motility and proliferation of GC cells by mechanisms involving the expression regulation of HDAC6, AC-tubulin, and cyclin D1.

Discussion

In this study, we first revealed that MIIP is downregulated in GC tissues and GC cell lines. Furthermore, ectopically expressed MIIP was found to significantly inhibit proliferation, colony formation, migration, and invasion of GC cells in vitro and in vivo. Our preliminary exploring on mechanisms underlying the negative correlation between MIIP expression and GC progression indicated that MIIP overexpression is associated with downregulated mRNA

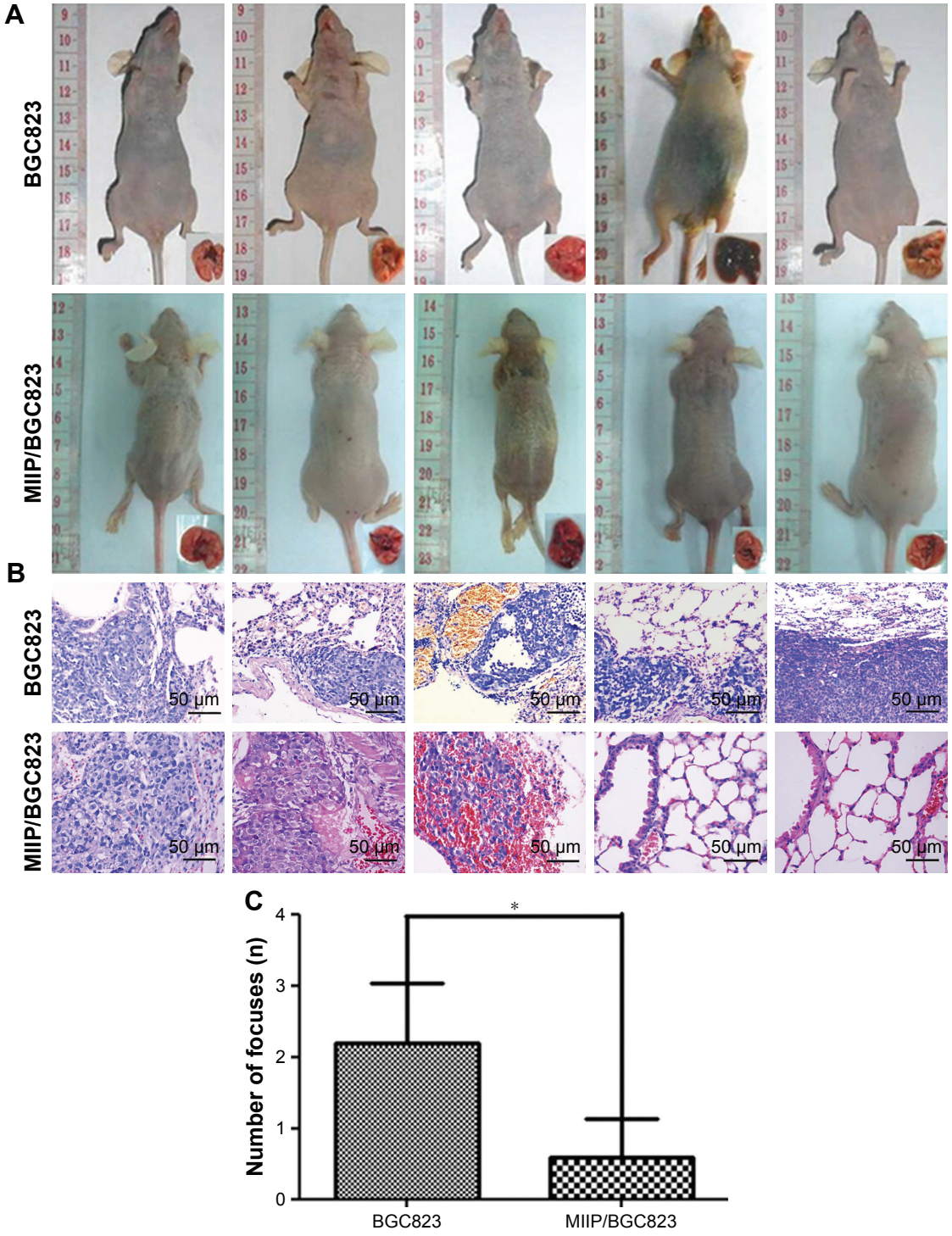

Figure 5 MIIP suppressed the metastasis of xenografted tumors to lung in the hematogenous dissemination mouse model of BGC823 cells.
Notes: (**A**) The hematogenous dissemination model was established by injecting BGC823 cells or MIIP/BGC823 cells into tail veins of BALB/c-nude mice. Mice lungs were harvested at 8 weeks after tumor inoculation. The photos of mice and their lungs are shown. (**B**) H&E staining of lung tissue sections indicated that the incidence of lung metastasis in the MIIP/BGC823 group (3/5, 60%) was obviously less than in the BGC823 control group (5/5, 100%). (**C**) The number of metastatic tumors in lung from the MIIP/BGC823 group was significantly fewer than that from the BGC823 group (*$P<0.05$).
Abbreviation: MIIP, migration and invasion inhibitory protein.

expressions of HOTAIR and MALAT1, elevated protein expression of AC-tubulin, and decreased protein expression of HDAC6 and cyclin D1. These data collectively suggest that MIIP acts as a suppressor in GC progression.

Previous studies have reported that MIIP was down-regulated in various carcinomas and plays as a putative suppressor gene in human tumor with diverse regulatory mechanisms. Wang et al revealed that both the mRNA

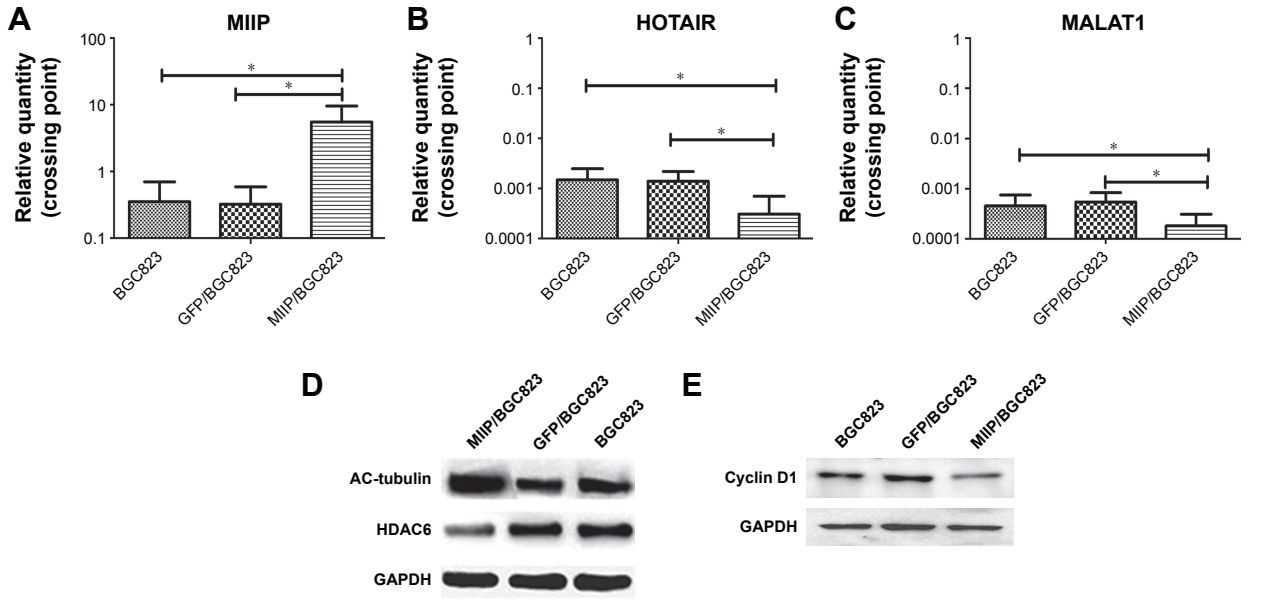

Figure 6 Ectopic expression of MIIP resulted in reduced expression of HOTAIR and MALAT1 transcripts and altered protein expression of AC-tubulin, HDAC6, and cyclin D1.

Notes: (**A**–**C**) As revealed by qRT-PCR assays in BGC823 cells, when the MIIP mRNA expression was remarkably elevated (**A**), the expressions of long noncoding RNAs HOTAIR (**B**) and MALAT1 (**C**) were obviously downregulated. (**D**, **E**) As revealed by Western blotting assays in BGC823 cells, overexpressing of MIIP unregulated the expression of AC-tubulin protein and downregulated the expression of HDAC6 protein and cyclin D1 protein. Data shown represent one of three experiments with similar results. *$P<0.05$.

Abbreviation: MIIP, migration and invasion inhibitory protein.

and protein expressions of MIIP were elevated in NSCLC in comparison with the paired normal tissues. Therefore, MIIP was considered as a tumor-suppressor gene of NSCLC development.[8] Furthermore, MIIP inhibited NSCLC cell proliferation by negatively regulating EGFR protein expression and accelerating EGFR protein turnover.[20] Moreover, it has been reported that the MIIP expression in endometrial cancer and advanced glioma tissues was also obviously downregulated, compared with their matched normal tissues, respectively.[6,7,10] In endometrial cancer, MIIP functioned as a tumor suppressor through weakening Rac1-signaling pathway, and loss of MIIP expression led to cytoskeleton reorganization and then increased the migration and metastasis of endometrial cancer cell.[10] In addition, MIIP was reported to antagonize insulin-like growth factor binding protein 2 to suppress glioma cell invasion.[21] MIIP consistently inhibits the expression of cell invasion-associated genes, such as the transcriptional NFκB, and its downstream target gene, intercellular adhesion molecule 1.[21] MIIP also directly interacted with Cdc20 to inhibit the cyclin B1 pathway,[7] and similarly, our work demonstrates that forced expression of MIIP decreased cyclin D1 expression. These data further substantiated the roles of MIIP in suppressing tumor growth at least partially through cell cycle regulation. It is worth noting that cell cycle-related molecules and signaling pathways, such as PTEN/Notch signaling,[22] PI3K/Akt signaling,[23] NEDD8-activating enzyme/P53,[24] and Wee1/P53,[25] have been identified as promising targets, just like MIIP, in treating GC and other cancers.

The MIIP expression has been previously reported to regulate tumor cell migration and invasion, as well as mitosis and tumorigenesis in various cancers. We also showed that ectopic expression of MIIP not only remarkably inhibited GC cell proliferation, colony formation, migration, and invasion but also induced tumor cell G0/G1 arrested in vitro. Furthermore, overexpressing MIIP significantly suppressed the growth and lung metastasis of xenografted tumors in vivo. Consistent with the majority of studies, MIIP played a suppressor role in GC. To the best of our knowledge, these findings revealed the effect of MIIP expression on GC progression for the first time. Notably, our analysis on database of 354 cases suggests that MIIP expression can predict better survival in patients with GC. As shown in Table 1, low expression of MIIP was found to only correlate to the anatomic neoplasm subdivision, but not to associate with depth of invasion, distant metastasis, and other clinicopathological features. This suggested that the impact of MIIP expression on the prognosis of GC patients was possibly mainly dependent on its long-term biological functions, but not on the pathological morphological factors

at one time. However, it deserves further study with involvements of more patients and their clinicopathological features at more time points.

However, another controversial study reported that the expression of MIIP in esophageal squamous cell carcinoma (ESCC) was obviously elevated, compared with matched paracancerous normal tissues.[26] Interestingly, MIIP expression was found to predict poor prognosis of resected ESCCs.[26] Therefore, the divergence on the roles of MIIP in tumor progression might be dependent on the cancer types. For example, the contribution of MIIP in adenocarcinoma and squamous cell carcinoma needs to be further elucidated.

Recently, a long noncoding RNA growth arrest specific 5 has been reported to attenuate the malignant biological properties of glioma stem cells by the miR-196a-5p–FOXO1–MIIP axis.[27] This study prompted us that there might be a crosstalk between the expressions of long noncoding RNA and MIIP. To test the hypothesis, we used qRT-PCR assay to evaluate the HOTAIR and MALAT1 expression in MIIP/BGC823 cells. Long noncoding RNA has been generally accepted as regulators of tumor formation and progression in various cancers.[28,29] HOTAIR and MALAT1 were two of most representative long noncoding RNAs in GC. Knockdown of HOTAIR expression significantly inhibited the abilities of invasion and migration in GC cells and resulted in tumor cell apoptosis and cell cycle arrest by decreased epithelial–mesenchymal transition-related protein expression.[15] MALAT1 also acts a biomarker for GC and promotes tumor cell proliferation, invasion, and metastasis by interacting with multiple signaling pathways.[30–32] In our study, there was a significant decrease of HOTAIR and MALAT1 expression in MIIP/BGC823 cells when comparing with control BGC823 and GFP/BGC823 cells. This suggests that MIIP overexpressing induced inhibition of GC invasion and metastasis are related to downregulation of HOTAIR and MALAT1. However, the exact mechanisms remain to be unveiled in the future. Nevertheless, our findings provided a new perspective for MIIP-related studies in GCs.

Cell motility is important for tumor cell migration and invasion, and it is controlled by the processes that modulate microtubule stabilization and destabilization cycles.[33,34] Acetylation of α-tubulin is one of the mechanisms involved in microtubule dynamics.[35] Members of the HDAC family regulate cell protein acetylation. Amplified HDAC6 expression has been discovered in various cancer cell lines and mouse tumor models.[36–38] HDAC6 is stably localized in the cytoplasm and specifically deacetylates α-tubulin, which is different from other HDAC family members.[36] MIIP directly binds HDAC6 to prevent remodeling of cytoskeleton by HDAC6.[39] Indeed, Wu et al found that MIIP could inhibit glioma migration through inhibition of HDAC6 and increased intracellular AC-tubulin levels.[12] In their study, the expression of HDAC6 increased while MIIP expression was lower in high-grade gliomas than lower-grade gliomas.[12] Furthermore, Ji et al showed that a siRNA against MIIP led to accelerated cell proliferation, while overexpression of MIIP in a glial-specific mouse model inhibited glioma progression.[7] In addition, they showed that MIIP overexpression attenuated mitotic transition and resulted in a higher incidence of mitotic catastrophe.[7] Latest study reported that the MIIP induced tumor progression through blocking HDAC6-mediated RelA deacetylation in colorectal cancer.[40] Giving these facts on the roles of HDAC6–AC-tubulin axis in progress of multiple tumors, we speculated that inhibition of HDAC6 and consequent increase of acetylated tubulin contribute significantly in MIIP overexpression-induced suppression of invasion and metastasis of GC cells.

Conclusion

For the first time, the current study has provided multiple lines of evidence in supporting that MIIP is a vital regulatory factor for GC progression. MIIP played a suppressor role in GC both in vitro and in vivo, which was associated with the dysregulated expressions of lncRNA HOTAIR and MALTA1, as well as HDAC6 and AC-tubulin. These findings suggest that MIIP is a new therapeutic target for treatment of GC. However, additional comprehensive exploration is still needed to further unveil the beneficial roles of MIIP modulation in GC.

Disclosure

The authors report no conflicts of interest in this work.

References

1. Strong VE, Wu AW, Selby LV, et al. Differences in gastric cancer survival between the U.S. and China. *J Surg Oncol*. 2015;112(1):31–37.
2. Rahman R, Asombang AW, Ibdah JA. Characteristics of gastric cancer in Asia. *World J Gastroenterol*. 2014;20(16):4483–4490.
3. Liang H, Kim YH. Identifying molecular drivers of gastric cancer through next-generation sequencing. *Cancer Lett*. 2013;340(2):241–246.
4. Al-Amri AM. Long-term survival of gastric adenocarcinoma without therapy: case report. *Oman Med J*. 2010;25(4):303–305.
5. Yang D, Hendifar A, Lenz C, et al. Survival of metastatic gastric cancer: significance of age, sex and race/ethnicity. *J Gastrointest Oncol*. 2011;2(2):77–84.
6. Song SW, Fuller GN, Zheng H, Zhang W. Inactivation of the invasion inhibitory gene IIp45 by alternative splicing in gliomas. *Cancer Res*. 2005;65(9):3562–3567.
7. Ji P, Smith SM, Wang Y, et al. Inhibition of gliomagenesis and attenuation of mitotic transition by MIIP. *Oncogene*. 2010;29(24):3501–3508.

8. Wang X, Liu H, Wang X, An Y. Clinical significance of migration and invasion inhibitor protein expression in non-small-cell lung cancer. *Oncol Lett*. 2014;8(6):2417–2422.
9. Sun Y, Ji P, Chen T, et al. MIIP haploinsufficiency induces chromosomal instability and promotes tumour progression in colorectal cancer. *J Pathol*. 2017;241(1):67–79.
10. Wang Y, Hu L, Ji P, et al. MIIP remodels Rac1-mediated cytoskeleton structure in suppression of endometrial cancer metastasis. *J Hematol Oncol*. 2016;9(1):112.
11. Song F, Zhang L, Ji P, et al. Altered expression and loss of heterozygosity of the migration and invasion inhibitory protein (MIIP) gene in breast cancer. *Oncol Rep*. 2015;33(6):2771–2778.
12. Wu Y, Song SW, Sun J, et al. IIp45 inhibits cell migration through inhibition of HDAC6. *J Biol Chem*. 2010;285(6):3554–3560.
13. Bertos NR, Wang AH, Yang XJ. Class II histone deacetylases: structure, function, and regulation. *Biochem Cell Biol*. 2001;79(3):243–252.
14. Okugawa Y, Toiyama Y, Hur K, et al. Metastasis-associated long non-coding RNA drives gastric cancer development and promotes peritoneal metastasis. *Carcinogenesis*. 2014;35(12):2731–2739.
15. Lee NK, Lee JH, Park CH, et al. Long non-coding RNA HOTAIR promotes carcinogenesis and invasion of gastric adenocarcinoma. *Biochem Biophys Res Commun*. 2014;451(2):171–178.
16. Lee NK, Lee JH, Ivan C, et al. MALAT1 promoted invasiveness of gastric adenocarcinoma. *BMC Cancer*. 2017;17(1):46.
17. Livak KJ, Schmittgen TD. Analysis of relative gene expression data using real-time quantitative PCR and the 2(-Delta Delta C(T)) method. *Methods*. 2001;25(4):402–408.
18. Stacey DW. Cyclin D1 serves as a cell cycle regulatory switch in actively proliferating cells. *Curr Opin Cell Biol*. 2003;15(2):158–163.
19. Masamha CP, Benbrook DM. Cyclin D1 degradation is sufficient to induce G1 cell cycle arrest despite constitutive expression of cyclin E2 in ovarian cancer cells. *Cancer Res*. 2009;69(16):6565–6572.
20. Wen J, Fu J, Ling Y, Zhang W. MIIP accelerates epidermal growth factor receptor protein turnover and attenuates proliferation in non-small cell lung cancer. *Oncotarget*. 2016;7(8):9118–9134.
21. Song SW, Fuller GN, Khan A, et al. IIp45, an insulin-like growth factor binding protein 2 (IGFBP-2) binding protein, antagonizes IGFBP-2 stimulation of glioma cell invasion. *Proc Natl Acad Sci U S A*. 2003;100(24):13970–13975.
22. Kim SJ, Lee HW, Baek JH, et al. Activation of nuclear PTEN by inhibition of Notch signaling induces G2/M cell cycle arrest in gastric cancer. *Oncogene*. 2016;35(2):251–260.
23. Jing X, Cheng W, Wang S, Li P, He L. Resveratrol induces cell cycle arrest in human gastric cancer MGC803 cells via the PTEN-regulated PI3K/Akt signaling pathway. *Oncol Rep*. 2016;35(1):472–478.
24. Wu KJ, Zhong HJ, Li G, et al. Structure-based identification of a NEDD8-activating enzyme inhibitor via drug repurposing. *Eur J Med Chem*. 2018;143:1021–1027.
25. Yang GJ, Zhong HJ, Ko CN, et al. Identification of a rhodium(iii) complex as a Wee1 inhibitor against TP53-mutated triple-negative breast cancer cells. *Chem Commun (Camb)*. 2018;54(20):2463–2466.
26. Wen J, Liu QW, Luo KJ, et al. MIIP expression predicts outcomes of surgically resected esophageal squamous cell carcinomas. *Tumour Biol*. 2016;37(8):10141–10148.
27. Zhao X, Liu Y, Zheng J, et al. GAS5 suppresses malignancy of human glioma stem cells via a miR-196a-5p/FOXO1 feedback loop. *Biochim Biophys Acta Mol Cell Res*. 2017;1864(10):1605–1617.
28. Zhang J, Zhang P, Wang L, Piao HL, Ma L. Long non-coding RNA HOTAIR in carcinogenesis and metastasis. *Acta Biochim Biophys Sin (Shanghai)*. 2014;46(1):1–5.
29. Yang L, Bai HS, Deng Y, Fan L. High MALAT1 expression predicts a poor prognosis of cervical cancer and promotes cancer cell growth and invasion. *Eur Rev Med Pharmacol Sci*. 2015;19(17):3187–3193.
30. Deng QJ, Xie LQ, Li H. Overexpressed MALAT1 promotes invasion and metastasis of gastric cancer cells via increasing EGFL7 expression. *Life Sci*. 2016;157:38–44.
31. Qi Y, Ooi HS, Wu J, et al. MALAT1 long ncRNA promotes gastric cancer metastasis by suppressing PCDH10. *Oncotarget*. 2016;7(11):12693–12703.
32. Zhang TH, Liang LZ, Liu XL, et al. Long non-coding RNA MALAT1 interacts with miR-124 and modulates tongue cancer growth by targeting JAG1. *Oncol Rep*. 2017;37(4):2087–2094.
33. Wehrle-Haller B, Imhof BA. Actin, microtubules and focal adhesion dynamics during cell migration. *Int J Biochem Cell Biol*. 2003;35(1):39–50.
34. Takemura R, Okabe S, Umeyama T, Kanai Y, Cowan NJ, Hirokawa N. Increased microtubule stability and alpha tubulin acetylation in cells transfected with microtubule-associated proteins MAP1B, MAP2 or tau. *J Cell Sci*. 1992;103(Pt 4):953–964.
35. Hammond JW, Cai D, Verhey KJ. Tubulin modifications and their cellular functions. *Curr Opin Cell Biol*. 2008;20(1):71–76.
36. Hubbert C, Guardiola A, Shao R, et al. HDAC6 is a microtubule-associated deacetylase. *Nature*. 2002;417(6887):455–458.
37. Sakuma T, Uzawa K, Onda T, et al. Aberrant expression of histone deacetylase 6 in oral squamous cell carcinoma. *Int J Oncol*. 2006;29(1):117–124.
38. Bazzaro M, Lin Z, Santillan A, et al. Ubiquitin proteasome system stress underlies synergistic killing of ovarian cancer cells by bortezomib and a novel HDAC6 inhibitor. *Clin Cancer Res*. 2008;14(22):7340–7347.
39. Wang Y, Wen J, Zhang W. MIIP, a cytoskeleton regulator that blocks cell migration and invasion, delays mitosis, and suppresses tumorogenesis. *Curr Protein Pept Sci*. 2011;12(1):68–73.
40. Chen T, Li J, Xu M, et al. PKCε phosphorylates MIIP and promotes colorectal cancer metastasis through inhibition of RelA deacetylation. *Nat Commun*. 2017;8(1):939.